Automated and enhanced extraction of a small molecule-drug conjugate using an enzyme-inhibitor interaction based SPME tool followed by direct analysis by ESI-MS

Working Paper

Author(s):
Ghiasikhou, Sahar; Cazzamalli, Samuele; Scheuermann, Jörg; Neri, Dario; Zenobi, Renato

Publication date:
2019

Permanent link:
https://doi.org/10.3929/ethz-b-000346473

Automated and enhanced extraction of a small molecule-drug conjugate using an enzyme-inhibitor interaction based SPME tool followed by direct analysis by ESI-MS

Sahar Ghiasikhou; Samuele Cazzamalli; Jörg Scheuermann; Dario Neri; Renato Zenobi*
Department of Chemistry and Applied Biosciences, ETH Zurich, 8093 Zurich, Switzerland

Corresponding Author

*E-mail: zenobi@org.chem.ethz.ch. Address: Prof. Renato Zenobi, Department of Chemistry and Applied Biosciences, ETH Zurich, CH-8093 Zürich, Switzerland. Tel: +41 44 632 4376. Fax: +41 44 632 1292.

ABSTRACT: We report a novel, fast and automatic SPME-based method capable of extracting a small molecule drug conjugate (SMDC) from biological matrices. Our method relies on the extraction of the drug conjugate followed by direct elution into an electrospray mass spectrometer (ESI-MS) source for qualitative and quantitative analysis. We designed a tool for extracting the targeting head of a recently synthesized SMDC, which includes acetazolamide (AAZ) as high-affinity ligand specific to carbonic anhydrase IX. Specificity of the extraction was achieved through systematic optimization. The design of the extraction tool is based on noncovalent and reversible interaction between AAZ and CAII that is immobilized on the SPME extraction phase. Using this approach, we showed a 330% rise in extracted AAZ signal intensity compared to a control, which was performed in the absence of CAII. A linear dynamic range from 1.2-25 µg/ml was found. The limits of detection (LOD) of extracted AAZ from phosphate-buffered saline (PBS) and human plasma were 0.4 and 1.2 µg/ml, respectively. This with a relative standard deviation of less than 14% (n=40) covers the therapeutic range.

Keywords: Capillary gap sampler; Solid phase microextraction; Targeted drug delivery; Small molecule-drug conjugates; Carbonic anhydrase; Acetazolamide.

❑ INTRODUCTION

The majority of anticancer drugs are designed to interfere with cell proliferation or survival events. However, chemotherapeutic agents often do not selectively accumulate in the tumor tissue after systemic administration. The unspecific biodistribution of anticancer drugs causes undesired toxicities in healthy organs and limits the therapeutic effectiveness of the drugs. Targeted delivery of potent cytotoxic agents to tumors represents a promising strategy to improve the therapeutic index and to limit undesired systemic toxicities. [1 - 4] In an attempt to improve drug efficacy, tumor-specific antibodies and small molecules have been proposed as selective delivery vehicles of toxic payloads to malignant cells. This approach led to the generation of new classes of drugs called Antibody-Drug Conjugates (ADCs) and Small Molecule-Drug Conjugates (SMDCs). The general structure of ADC and SMDC products includes a therapeutic payload attached to a ligand specific to a marker of disease, through a spacer that often contains a cleavable bond. [2] In this way, the drug will accumulate and act at the intended site of action, therefore increasing the efficiency of the applied dose, while side effects for the healthy cells decrease. Different targeting moieties have been proposed, including tumor-specific antibodies, [5, 6] aptamers, [7 - 9] peptides [10 - 13] and low-molecular weight non-peptidic ligands. [14 - 17] The use of antibodies as targeting head has several limitations: antibodies are large molecules, and thus have problems penetrating deeply into solid tumors. [18] Other disadvantages are the drug's long circulation times. [19] This has shifted the focus to small molecule drugs, as they have advantages in terms of pharmacokinetics, [10] in vitro and in vivo stability, [20] antigenicity, [21, 22] conjugate chemistry and cost of manufacturing. Folate Receptor, [23] Prostate Specific Membrane Antigen, [24] Somatostatin Receptors, [25] and Carbonic Anhydrase IX, [26] have been successfully targeted with small molecules.

Carbonic anhydrase IX (CAIX) is a metalloenzyme and transmembrane protein involved in cell adhesion, pH homeostasis, and upregulated by hypoxia during tumor development and progression. The excellent tumor-targeting performance of AAZ, a small organic ligand for CAIX, was demonstrated by quantitative biodistribution in a murine model of Renal Cell Carcinoma. [26] AAZ showed good tumor-penetrating properties and fast targeting kinetics. AAZ derivatives of cytotoxic payloads have been generated and characterized for their potent in vivo anti-tumor activity against Carbonic Anhydrase IX expressing solid tumors in mice. Chemically defined ADC and SMDC products targeting CAIX have been generated and compared in terms of tumor-homing properties and therapeutic effect. [27] In quantitative biodistribution experiments performed with radiolabeled drugs administered intravenously to tumor bearing, the small organic ligand showed about 40% injected dose per gram (%ID/g) 6 hours after injection, while the anti-CAIX antibody only displayed a 4%ID/g after 24 hours. Moreover, fluorescently labeled SMDC and ADC were analyzed for their diffusion properties in solid tumors. While the antibody-based product only localized nearby vascular structures, the anti-CAIX small ligand homogeneously accumulated over the tumor mass in a very short period of time (1 h after injection). Therapy experiments indicated potent antitumor effect of both ADC and SMDC products. In order to evaluate the targeting performance, experiments that do not require labeling and modification of the drugs are required. This might simplify sample preparation and lower generation of experimental artifacts. There is also a great demand for techniques capable of quick, site specific and low-volume sample analysis, which would render the drug biodistribution screening in the tissue possible.

In this article, we report the development of a label-free SPME-based method, which allows analysis of the of anti-CAIX SMDCs in biological matrixes. We present the capillary gap sampler as a platform for direct coupling of site-specific solid phase microextraction with ESI-MS. Using such a sampler, SMDC products can be selectively and quickly extracted from low volumes of different matrices and later quantified by ESI-MS analysis. The extraction step is based on the interaction between immobilized CAII, a commercially available and inexpensive isoform of CA, and the targeting moiety of anti-CAIX SMDCs.

❑ MATERIALS AND METHODS

Chemical and Materials. Acetonitrile≥99.9% (LC-MS CHROMASOLV), water (LC-MS grade), bovine carbonic anhydrase II, human plasma, bovine serum albumin, myoglobin Dimethyl sulfoxide (for acetazolamide solution preparation) were purchased from Sigma Aldrich (St Louis, MO, USA). Also, diazepam and diazepam-d5 were obtained from Sigma Aldrich (The Woodlands, TX, USA) and stored at 4°C. Acetazolamide ≥99% and Methazolamide ≥98% were purchased from Sigma (Steinheim, Germany). Methanol and ethanol (HPLC grade) were purchased from Fisher Scientific (Loughborough, U.K). Formic acid (98-100%) and rhodamine B were purchased from Merck (Darmstadt, Germany). Acetone was provided by Aldrich (Milwaukee, WI, USA). Dynabeads M-270 Epoxy was purchased from Thermo Fisher Scientific (Baltics, Norway) and stored at 2-4°C. 8-Anilino-1-naphthalenesulfonic acid was bought from Fluka-Chemie AG (Buchs, Switzerland). Polyacrylonitrile (PAN), which was used as a biocompatible glue to immobilize the beads on the stainless-steel pin, was purchased from Acros (New Jersey, USA). AAZ-VC-MMAE was synthesized as described in Ref. [28].

Equipment for detection (Mass Spectrometer), software, buffer delivery. A Synapt G2-S high definition mass spectrometer (Waters, Manchester) operated in positive ion mode was used for the experiments. The source temperature was set to 30°C and the capillary voltage to 3.3 kV. Masslynx 4.1 software was used for acquiring the data. Buffer delivery was performed via a syringe pump (neMesys, Cetoni, Korbuss, Germany).

Sampler Design. The capillary gap sampler allows direct hyphenation of a miniaturized sampling device to ESI-MS. Its main compartments are a sampling tool and a microfluidic platform as the sample receptor. The entire setup is 4.5 kg and is fixed to the front part of the MS. The sampling tool serves to extract and deliver the sample into a liquid junction inside the microfluidic chamber. This chamber (V= 0.65 ml) is made of PEEK and held under a controlled overpressure. Inside the chamber, which is the heart of the sampler, two capillaries face each other with a gap of about 200-300 µm where a liquid bridge of 10-40 nanoliters forms. The liquid bridge is built up when a solution is delivered by a syringe and flows through the first fused silica capillary (360 µm O.D.; 50 µm I.D., Polymicro, Phoenix, AZ, USA). This liquid then fills the gap between the two capillaries and enters the second stainless steel capillary (320 µm O.D.; 50 µm I.D.; 50 mm length; New Objective, Woburn, MA, USA). The second capillary also acts as the direct ESI spray needle in front of the MS inlet. Alternatively, a single capillary with a hole can be used as the sample receptor. This yields higher sensitivity, robustness and ability to work with high surface tension solutions. More details can be found in previous publications by Ghiasikhou et al. [29] and Neu et al. [30].

The sampling tool is a solid stainless-steel pin, which picks up a small droplet of the sample by dipping into a microwell. This pin is held and moved by a light microrobot (model PocketDelta, Asyril, Villaz-St-Pierre, Switzerland) with fast, pulsation free and precise movement (3µm). The sample delivery step is monitored by a CCD camera (model µ-eye, VS Technology Cooperation, Tokyo, Japan) and Telocentric optics (VS Technology Cooperation).

Workflow for sample extraction and elution

1) Loading: in this step, the extraction tool is dipped into the sample solution and binds with the analyte of the interest noncovalently (Fig. S1 in supplementary information). CAII and AAZ were found to bind best at a pH of ~7.2 (Fig. S2 in supplementary information) The rate of extraction increases by performing agitation in this step. This is achieved by quick movements of the extraction tool inside the sample well. [31]

2) Washing: this refers to the step of removing the remaining matrix off the pins, with minimum loss of the analyte of interest. In this case, washing occurs in water at a pH of 7.4.

3) Elution: this is the step of desorption of the analyte using an appropriate elution solution. Using the capillary gap sampler, elution is performed inside the liquid bridge. The eluted compound is then sprayed directly into the MS inlet. The extraction tool is left in the gap exposed to the desorption solution for 2 minutes, until the extracted ion chromatogram signal has reached baseline level again (explained in Fig. 5).

4) Conditioning: after the elution step and prior to the next round of the experiment, the extraction tool moves into water at a pH of 7.4 to keep the CAII folded.

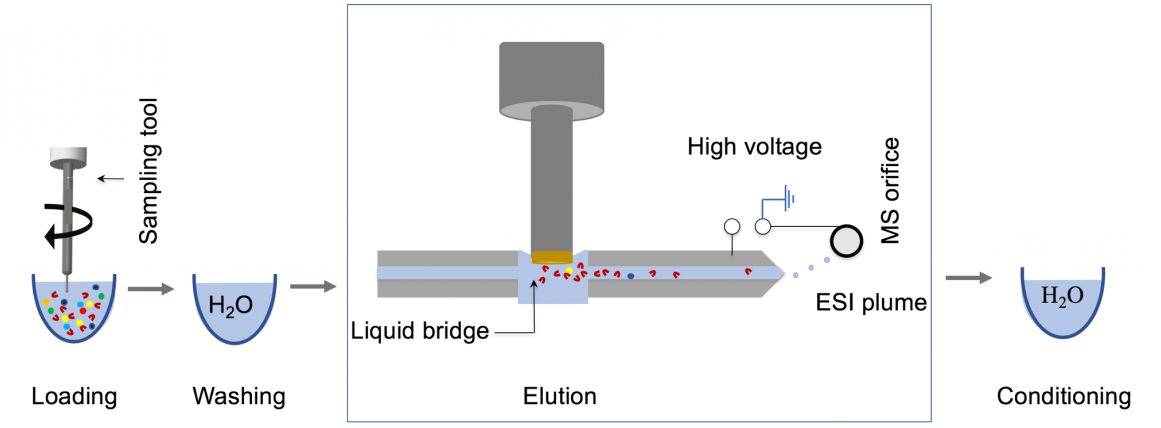

Figure1. In this figure extraction workflow including loading, washing, elution, conditioning is shown. The elution step happens in the formed liquid bridge in between two capillaries.

Preparation of the SPME tool. The stainless-steel pin was washed and sonicated with isopropanol/methanol, followed by a O_2 plasma cleaning procedure. Silica beads carrying epoxide functionalization on their surface were then fixed to the metal tip using polyacrylonitrile (PAN) polymer, and this PAN glue was later cured in the oven at 180°C for two minutes. After cooling down to room temperature, the epoxy-modified beads were incubated in CAII for 48 hours at 2-4°C. The CAII was immobilized on the beads through an amine-epoxy reaction. The unreacted

active epoxy groups were quenched by incubation in Tris 20 mM buffer for half a day. A SEM image of the coated extraction tool is shown in Fig.2.

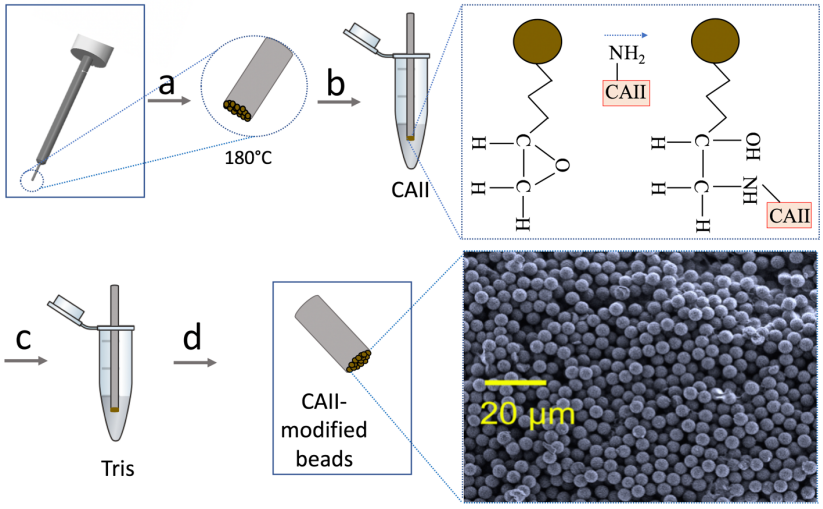

Figure 2. Extraction tool preparation steps, a) gluing epoxy-modified beads onto the solid pin and curing at 180°C, b) incubation with CAII and amine-epoxy reaction, c) incubation in Tris buffer, d) SEM image of the CAII-modified beads after immobilization on the extraction tool, confirming that beads are not covered with PAN glue.

❑ RESULTS AND DISCUSSION

Proof of CAII immobilization. In order to evaluate whether the immobilization of CAII on the epoxy beads was successful, a well-established protein identification test with 8-anilinonaphthalene-1-sulfonic acid (ANS) was performed. ANS is a hydrophobic organic dye containing both a sulfonic acid and an amine group. Non-covalent binding of ANS and peptides/proteins in solution largely occurs through the negatively charged sulfonate groups and the positively charged side chains of the arginine residues of the proteins. [32, 33] Fluorescence enhancement results from ion paring between the arginine from CAII with the ANS sulfonate group. [34] In this test, epoxy-modified beads were glued onto two microscope slides (one as a control experiment) and incubated with a buffer solution with and without CAII for 48 hours at 4°C. In order to remove non-specifically bonded ANS while keeping proteins in their correct folding, beads were rinsed with water, incubated with an ANS solution for one hour and washed with saline buffer at pH 7.4 to remove any non-specifically bonded ANS while the proteins were kept folded. Both slides were observed under a fluorescent microscope. Several areas were imaged using both the blue fluorescence emission channel and bright field modes. The results are shown in Fig. 3.

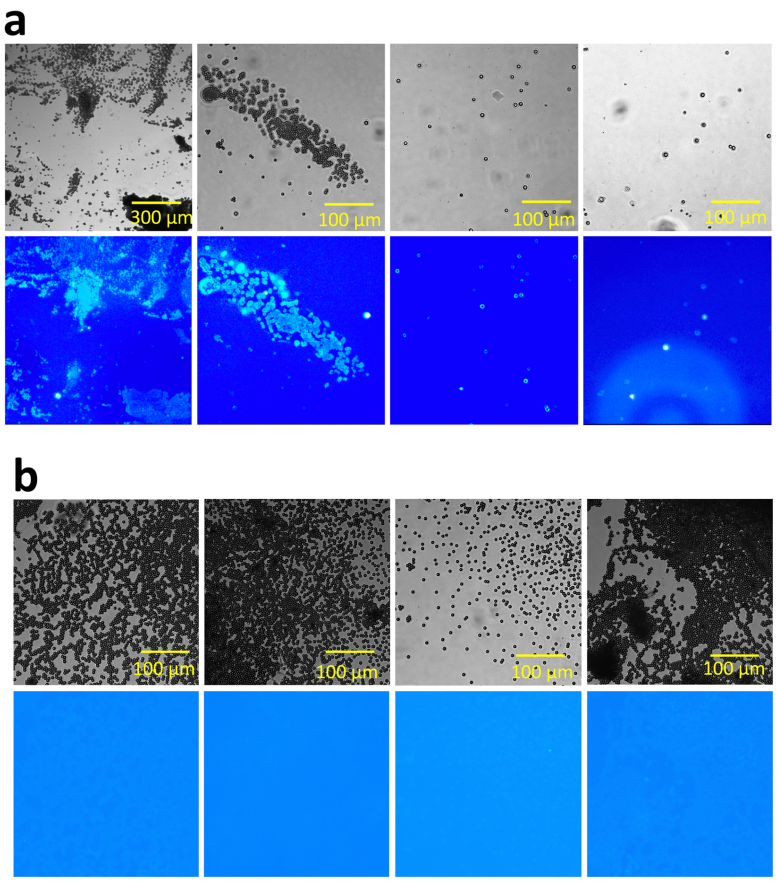

Figure 3. Bright field and blue channel images from the epoxy-modified beads (incubated a) with, b) without CAII) after reacting with ANS.

The results shown in Fig. 3 confirm the binding of CAII to the beads. Images were selected from areas with different bead densities. Comparison of the fluorescent enhancement among series a and b confirms the presence of CAII proteins on the beads in Fig. 3a.

Influence of the desorption solution on the acetazolamide signal. Selection of the right desorption solution is crucial to have a complete elution of the analyte and to keep the CA protein properly folded for the next extractions. In order to separate the analyte from the enzyme, different mixtures of organic solvents acetonitrile, methanol, ethanol and acetone and water were tested. Restrictions such as the pH or organic solvent content of the mixture should be considered. Decreasing the pH or increasing the organic solvent-to-water ratio of the solution increases the release of the inhibitor from CAII, but also increases the probability of protein denaturation. On the other hand, the stability of the liquid bridge in the double capillary system is significantly enhanced by increasing the organic ratio of the mixture. The reason is their low surface tension in comparison with water. Possible denaturation during the elution process can be overcome by placing the extraction tool in a buffer solution with physiological pH immediately after elution and prior to the next extraction (conditioning step). Solutions containing 50% of the mentioned organic solvent and water, plus 0.1% formic acid for enhancing ionization were prepared. Methazolamide

(1 μM) was added to the solution in order to normalize the acetazolamide signal intensity. Extraction of acetazolamide 5μM from PBS was performed 10 times for each solution. Results are shown in Fig. 4.

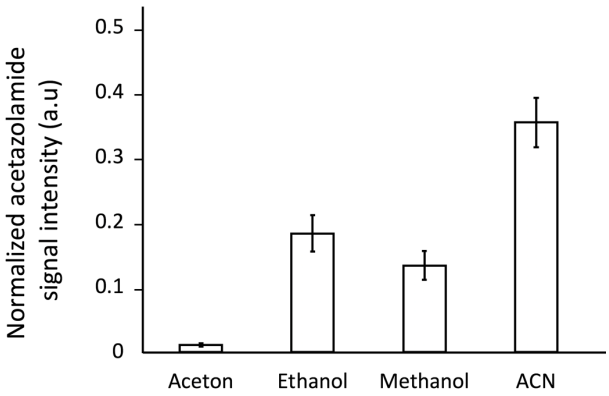

Figure 4. Average amount of eluted acetazolamide (n=10) using acetonitrile, methanol, ethanol and acetone 50% mixed with water (plus 0.1% of formic acid) as the desorption solution. The results are normalized to methazolamide (1 μM).

As shown in Fig. 3, water containing 50% acetonitrile elutes more acetazolamide compared to the other organic solvents, which can be explained by the higher solubility of AAZ in ACN and its lower pH value in comparison with other solutions. The use of 50% ACN also results in a smaller RSD, most probably due to lower carry-over from the previous 120 seconds of elution. We also expected the protein to be more prone to becoming denatured after dissociation of the acetazolamide. This expectation is supported by a study by Almstedt et al. [35] who showed that sulfonamide ligands, bound to the metal cofactor (the active site of the enzyme), can further stabilize CA against denaturation. Therefore, after acetazolamide elution, CAII is more prone to denaturation, i.e., long elution times should be avoided. Considering our experimental parameters, such as coating thickness, acetazolamide concentration, etc., and in accordance with the extracted ion chromatogram of the acetazolamide, a 2-minute elution was found to be enough for the chromatogram to return to baseline. An example of an extracted ion chromatogram of acetazolamide is shown in Fig. 5, which confirms that 2 minutes is long enough for the elution step.

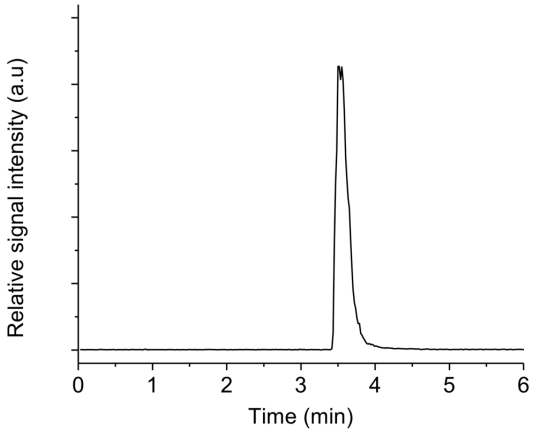

Figure 5. Extracted ion chromatogram of acetazolamide (20 μM) after extraction from PBS.

In order to confirm that CAII is not denatured during the desorption step, CAII 20 µM was incubated in 50 % ACN: H2O for 2 minutes and sprayed directly into MS using borosilicate nano-emitters. Figure 6 represents the resulting spectrum. The peaks marked in Fig. 6 correspond to a native charge state distribution of CAII, thus confirming the high stability of CAII against denaturation in 50 % ACN: H_2O.

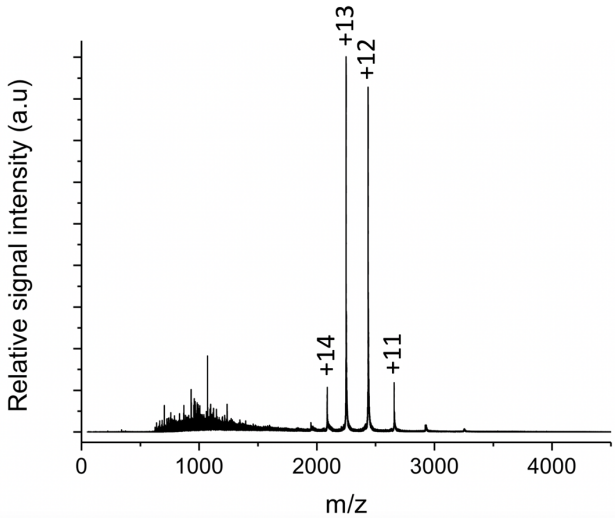

Figure 6. The nano-ESI spectrum of CAII 20 µM incubated in 50 % ACN: H_2O for 2 minutes.

Extraction of AAZ-VC-MMAE from human plasma by the capillary gap sampler. After understanding and optimizing different experimental parameters such as pH, desorption solution and time, an evaluation of the technique for drug extraction was performed. A solution of AAZ-VC-MMAE of 2.5 µg/ml was directly sprayed by a borosilicate nano-emitter, and the spectrum shown in Fig. 7a was collected. Then, using a CAII modified pin, the 2.5 µg/ml drug was extracted from PBS (Fig. S4b, supplementary information) and human plasma (Fig. 7b). The human plasma was spiked with the drug and left overnight in the fridge at 2-4°C. A control experiment was performed, in which 2.5 µg/ml AAZ-VC-MMAE was extracted from PBS using bare beads (Fig. S4a). The results are shown in Fig. 7. The peaks corresponding to the drug are marked in the spectra.

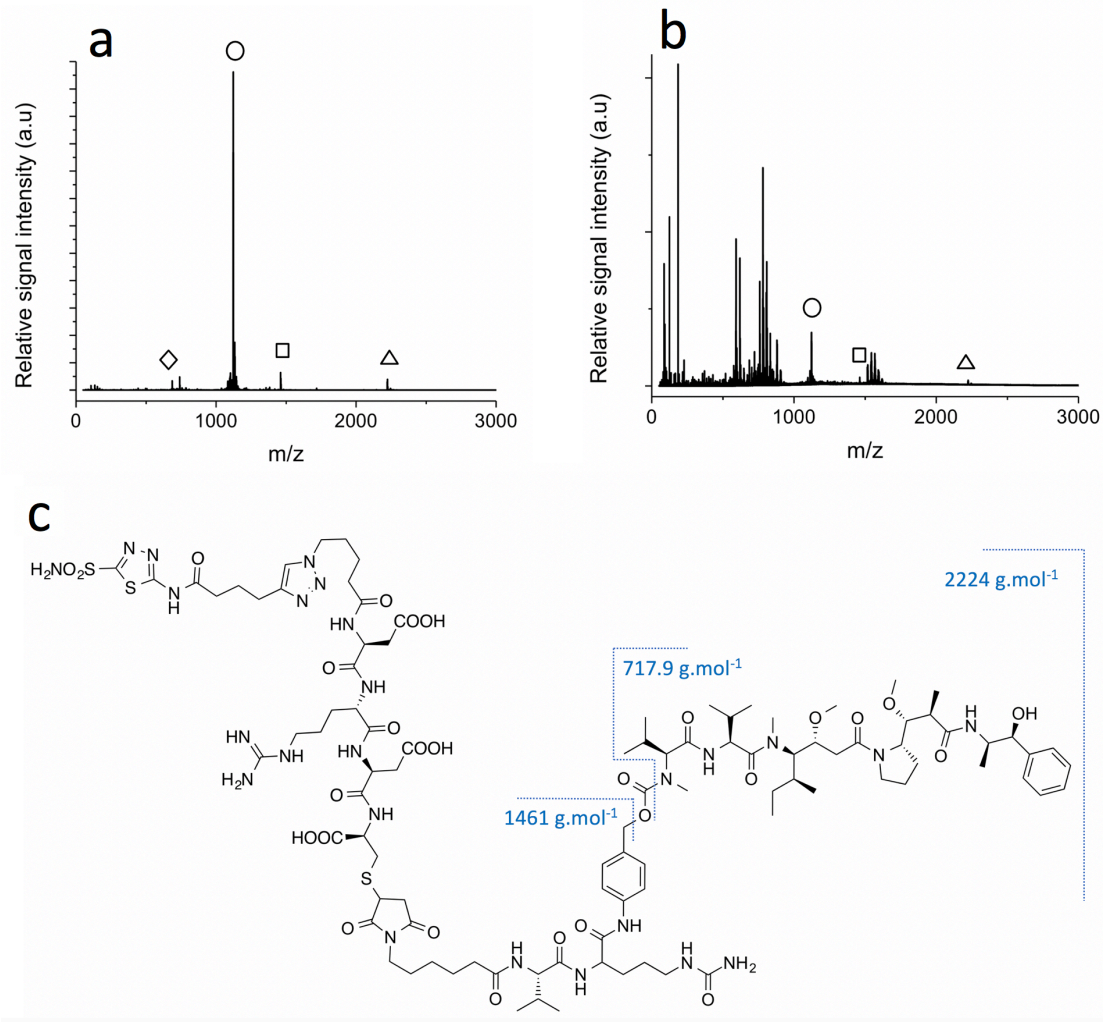

Figure 7. Spectrum of AAZ-VC-MMAE, a) direct infusion by nanospray, b) extraction from human plasma. The following peaks were observed in both spectra: (◇) MMAE+ H^+=718.51 m/z, (○) AAZ-VC-MMAE+ $2H^+$=1113.03 m/z, (○) AAZ-VC-MMAE+H^++Na^+ =1123.53 m/z, (□) AAZ-VC-MMAE – MMAE – CO_2 =1461, (△) AAZ-VC-$MMAE^+$=2224.05m/z. Part c shows the chemical structure of AAZ-VC-MMAE.

Five identical peaks in both spectra indicate the success of the drug extraction from human plasma. Peaks between 50 and 800 m/z mostly originate from the coating glue of the extraction tool, and some from human plasma. For example, the strong peaks at 780.7 and 591.7 m/z were observed while extracting from both PBS (Fig S4) and human plasma, therefore they must originate from the coating material. The peaks observed at 718.51, 1113.03, 11123.53, 1461 and 2224.05 m/z correspond to MMAE+ H^+, AAZ-VC-MMAE+ $2H^+$, AAZ-VC-MMAE+H^++Na^+ AAZ-VC-MMAE – MMAE – CO_2, and AAZ-VC-$MMAE^+$, respectively. Extraction of the drug from human plasma is more challenging due to matrix effects: firstly, unspecific adsorption of macromolecules to the beads' surfaces and pores, and competition between the proteins in the plasma and the extraction phase for the drug can occur. The second point depends strongly on the differences of the competitor's (extraction phase and plasma) affinity for the target analyte and the concentration of each.

Specificity of the extraction. The specific extraction approach is crucial to discriminate against other compounds in a biological sample. In this context, the term specific means enhancing the extraction of the analyte of interest as much as possible while minimizing interferences from unwanted compounds, to make the data interpretation as clean and simple as possible. In most cases, nonspecific extraction cannot be avoided but can be minimized. To investigate the specificity of the AAZ extraction, three different proteins including CAII, BSA and myoglobin, were immobilized on the extraction tool. Then, using these three pins and a pin without immobilized protein (as a control), seven extractions of acetazolamide 6.7 M from PBS were performed. Results are plotted in Fig. 8.

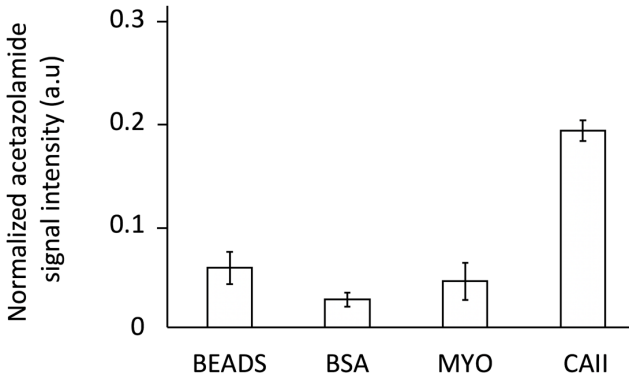

Figure 8. Extraction of acetazolamide using three different proteins (bovine serum albumin, myoglobin and carbonic anhydrase II) immobilized on the pins, plus a control experiment (bare beads). The acetazolamide signal intensities are normalized to methazolamide 2 μM. (n=7)

Although nonspecific binding was observed for all the pins, extraction was significantly enhanced using CAII modified beads, which means that carbonic anhydrase II binds AAZ specifically and therefore provides an enhanced extraction. Nonspecific binding can be minimized by a longer washing time after extraction and prior to the desorption step. Epoxy-modified beads are hydrophilic and pH neutral. AAZ is also hydrophilic, which explains the nonspecific extraction in the control experiment. Immobilization of BSA and myoglobin render the surface more hydrophobic and they do not bind AAZ specifically, therefore less extraction of AAZ was observed. In another test, extraction of AAZ from a mixture of different analytes using a CAII modified pin was evaluated. The mixture consisted of three compounds, acetazolamide, diazepam and MMAE, each at a concentration of 6.7 μM in PBS.

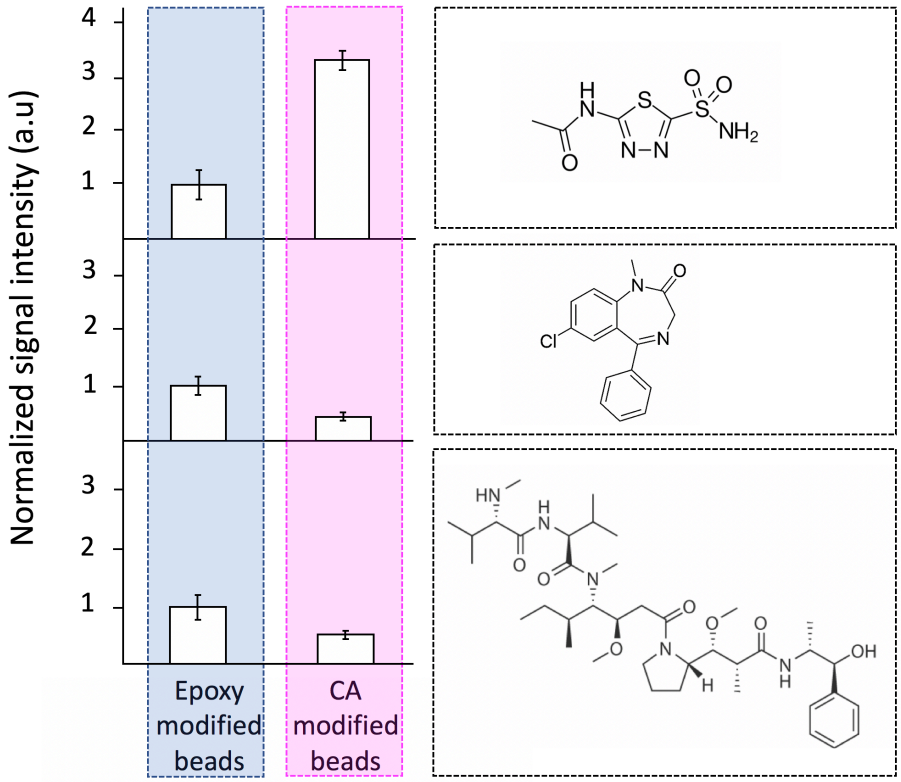

Figure 9. Comparison of the extraction of three different analytes, a) acetazolamide, b) diazepam, c) MMAE, using CAII and epoxy-modified beads. (n=5)

Fig. 9 shows the results. For each analyte peak, intensities were normalized to the analyte intensity extracted by the epoxy-modified beads. The normalized intensity of the peaks is compared for each extracted analyte using CAII modified pins, plus a control using bare epoxy-modified beads. According to Fig. 9, modification of the pin with CAII greatly enhances the extraction of acetazolamide and decreases the extraction of diazepam and MMAE. The high affinity of CAII to acetazolamide is the main reason for the 330% enhancement of the extraction.

Time profile of the extraction. The concept of SPME was developed to address the need for fast sample cleanup. The SPME extraction phase is in contact with the sample matrix for a well-defined amount of time. Depending on several factors such as temperature, the affinity of the extraction phase with the analyte, the volume of the extraction phase and sample volume, analyte concentration, and agitation, the amount of the extracted sample may vary. The extraction strategy can either be designed on the basis of pre-equilibrium or equilibrium conditions. The former is accomplished by stopping extraction before equilibrium has been reached. In the equilibrium-based approach, convection/agitation conditions do not affect the extracted amount. However, when using the pre-equilibrium method, high reproducibility, which is especially important for the purpose of quantification, can be achieved only if convection/agitation is controlled. Pre-equilibrium extraction is quicker compared to equilibrium-based extraction and, pending acceptable level of sensitivity, accuracy and reproducibility, it would be the preferred method. In this section, several extractions from a 20 µM acetazolamide solution in 40 µL PBS were performed by a CAII modified

pin. The extraction time was varied to find the equilibration time. Each experiment was repeated 3 times. Agitation was performed in all the extractions. The time profile of the extraction is shown in Fig. 10.

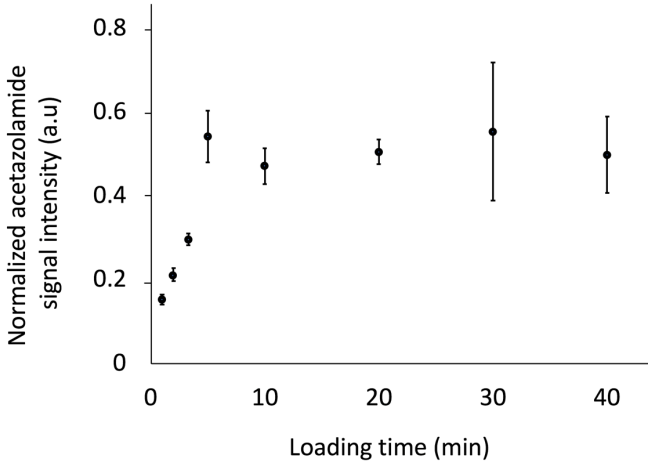

Figure 10. The time profile of the extraction acetazolamide (20 µM) from PBS. (n=3) The results are normalized to methazolamide (2 µM).

By increasing the extraction time, the signal intensity of the extracted acetazolamide increases. This increase continues for the first five minutes, after which no considerable change is observed. Therefore, equilibrium is reached within five minutes in this case. The equilibrium is determined by the distribution constant K_{es} for a solid extractant defined as $K_{es} = S_e / C_s$, [36] where S_e is the surface concentration of the adsorbed analyte on the extraction phase and C_s is the analyte concentration in the sample. The sorbent surface area is also considered in the definition of S_e. Thus, for a higher surface-to-volume ratio, equilibrium is reached faster, i.e. this method can be designed for high-throughput screening where speed and time are important factors. An efficient agitation technique during extraction reduces the equilibration time by making the boundary layer thinner. [37, 38]

AAZ extraction linearity, sensitivity, limit of detection, and recovery. One of the advantages of SPME-based methods over traditional sample preparation methods is their ability to quantify total concentration of a drug in a biological fluid or tissue. According to the therapeutic concentration of acetazolamide in human plasma, which is about 5-10 µg/ml, [39] the linear dynamic range range and limit of detection should be evaluated. Equilibrium-based extraction of the acetazolamide is shown in Fig. S3. Linearity was found over the entire calibration range of 1.2-25 µg/ml, with a regression coefficient of 0.997, which is more than the therapeutic range. For a signal-to-noise ratio of 3:1, the LOD was 400 ng/l from PBS and 1.2 µg/ml from human plasma, respectively. In another set of experiments, different concentrations of acetazolamide were sprayed into the MS inlet. From these data, a calibration curve was constructed and the recovery of the equilibrium-based extraction was calculated. Recovery of the extractions was found to be 5%. In accordance with the therapeutic range and achieved LOD, this method provides enough sensitivity for acetazolamide quantifications.

Repeatability. To confirm the repeatability of the extraction, forty tests were performed. In each test, 500 nM acetazolamide was extracted from PBS solution.

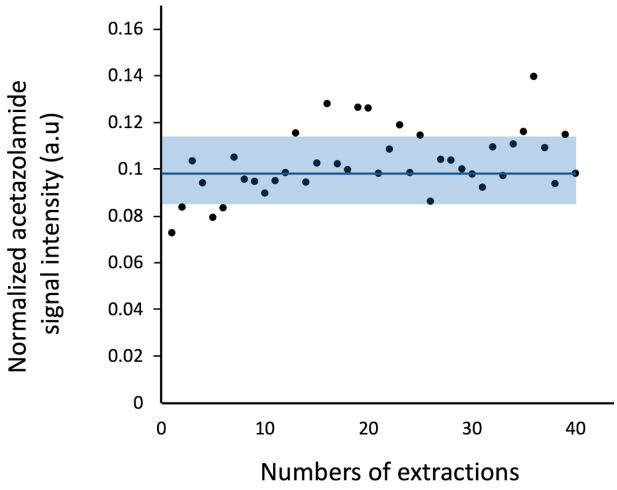

Figure 11. Repeatability test. RSD for forty extractions of 500 nM acetazolamide from PBS was found to be 13.5%. The solid blue line represents the means value. The data were normalized to methazolamide (200 nM).

The relative standard deviation of 13.5% for forty extractions represents an acceptable reproducibility of the process.

❑ CONCLUSIONS AND OUTLOOK

In this paper, we describe a novel affinity solid phase micro extraction tool with the aim of improving the capabilities of SPME. We presented CAII protein as the extraction phase for affinity extraction of an acetazolamide-based SMDC product capable of selective localization to CAIX-positive tumors. The procedure and proof of immobilization are demonstrated. The critical steps of analyte elution were studied. The desorption solution was optimized to efficiently elute the highest possible amount of the extracted sample and to keep the protein in its active folded structure. The specificity of the extraction was studied in a two-step evaluation. Firstly, acetazolamide was extracted using different protein-modified beads, and in the second approach, using CAII modified beads, acetazolamide was extracted from a mixture. Using both approaches, extraction using CAII modified beads showed considerable enhancement in the affinity extraction of acetazolamide. Further experiments on extraction performance were applied. In accordance with available biodistribution data of acetazolamide-based compounds, this model proved to be sensitive enough to satisfy the requirements related to linearity range and detection limit. On the other hand, the unique design of the sampler provides precise and fast movement of the extraction tool, which makes it potentially useful for analyzing tissue for future bioimaging applications. As an example, it can be interesting for the evaluation of targeted drug delivery performance. After a certain time from the injection of the drug, the targeted tissue can be collected and drug distribution can be monitored. This specific extraction approach is critical in order to minimize the interference from the biological sample being investigated. In future the method can be used for in vivo applications and biocompatible specific coatings could be developed including specific affinity phases for a range of important target analysis.

❑ ACKNOWLEDGMENTS

We gratefully thank Dr. Christof Fattinger (Roche) for his support in sampler development. Moreover, we thank the Scientific Center for Optical and Electron Microscopy (ScopeM), a central technology platform of ETH Zurich, for providing us with resources and services in electron microscopy. Finally, we thank the Swiss National Science Foundation (SNSF) for funding this project (Grant numbers 200020-159929 & 200020-178765).

❑ ASSOCIATED CONTENT

*S Supporting Information

This material is available free of charge via the Internet at…

The original data used in this publication are made available in a curated data archive at ETH Zurich (https://www.researchcollection.ethz.ch) under the 10.3929/ethz-b-000334909.

❑ REFERENCES

1. Krall N, Scheuermann J, Neri D (2013) Small targeted cytotoxics: current state and promises from DNA-encoded chemical libraries. Angew Chem Int Ed Engl 52:1384–1402. doi: 10.1002/anie.201204631

2. Srinivasarao M, Galliford CV, Low PS (2015) Principles in the design of ligand-targeted cancer therapeutics and imaging agents. Nature Reviews Drug Discovery 14:203–219. doi: 10.1038/nrd4519

3. van der Veldt AAM, Hendrikse NH, Smit EF, Mooijer MPJ, Rijnders AY, Gerritsen WR, van der Hoeven JJM, Windhorst AD, Lammertsma AA, Lubberink M (2010) Biodistribution and radiation dosimetry of 11C-labelled docetaxel in cancer patients. Eur J Nucl Med Mol Imaging 37:1950–1958. doi: 10.1007/s00259-010-1489-y

4. van der Veldt AA, Lubberink M, Mathijssen RH, Loos W, Herder GJ, Greuter HN, Comans EF, Rutten H, Eriksson J, Windhorst AD, Hendrikse H, Postmus PE, Smit EF, Lammertsma AA (2013) Towards prediction of efficacy of chemotherapy: a proof of concept study in lung cancer patients using [11C] docetaxel and positron emission tomography. Clin Cancer Res clincanres.3779.2012. doi: 10.1158/1078-0432.CCR-12-3779

5. van der Meel R, Vehmeijer LJC, Kok RJ, Storm G, van Gaal EVB (2016) Ligand-targeted Particulate Nanomedicines Undergoing Clinical Evaluation: Current Status. In: Prokop A, Weissig V (eds) Intracellular Delivery III: Market Entry Barriers of Nanomedicines. Springer International Publishing, Cham, pp 163–200

6. Ravi VJ, Miller ML, Widdison WC (2014) Antibody–Drug Conjugates: An Emerging Concept in Cancer Therapy. Angew Chem Intern Ed. 53:3796-3827. doi: 10.1002/anie.201307628.

7. Wang AZ, Farokhzad OC (2014) Current Progress of Aptamer-Based Molecular Imaging. J Nucl Med 55:353–356. doi: 10.2967/jnumed.113.126144

8. Zhang X, Zhang J, Ma Y, Pei X, Liu Q, Lu B, Jin L, Wang J, Liu J (2014) A cell-based single-stranded DNA aptamer specifically targets gastric cancer. The International Journal of Biochemistry & Cell Biology 46:1–8. doi: 10.1016/j.biocel.2013.10.006

9. Yu B, Tai HC, Xue W, Lee LJ, Lee RJ (2010) Receptor-targeted nanocarriers for therapeutic delivery to cancer. Molecular Membrane Biology 27:286–298. doi: 10.3109/09687688.2010.521200

10. Kurzrock R, Gabrail N, Chandhasin C, Moulder S, Smith C, Brenner A, Sankhala K, Mita A, Elian K, Bouchard D, Sarantopoulos J (2012) Safety, Pharmacokinetics, and Activity of GRN1005, a Novel Conjugate of Angiopep-2, a Peptide Facilitating Brain Penetration, and Paclitaxel, in Patients with Advanced Solid Tumors. Mol Cancer Ther 11:308–316. doi: 10.1158/1535-7163.MCT-11-0566

11. Zhang X-X, Eden HS, Chen X (2012) Peptides in cancer nanomedicine: Drug carriers, targeting ligands and protease substrates. Journal of Controlled Release 159:2–13. doi: 10.1016/j.jconrel.2011.10.023

12. Rana S, Nissen F, Lindner T, Altmann A, Mier W, Debus J, Haberkorn U, Askoxylakis V (2013) Screening of a Novel Peptide Targeting the Proteoglycan-Like Region of Human Carbonic Anhydrase IX. Mol Imaging 12:7290.2013.00066. doi: 10.2310/7290.2013.00066

13. McGuire MJ, Gray BP, Li S, Cupka D, Byers LA, Wu L, Rezaie S, Liu Y-H, Pattisapu N, Issac J, Oyama T, Diao L, Heymach JV, Xie X-J, Minna JD, Brown KC (2014) Identification and Characterization of a Suite of Tumor Targeting Peptides for Non-Small Cell Lung Cancer. Scientific Reports 4:4480. doi: 10.1038/srep04480

14. Xia W, Low PS (2010) Folate-Targeted Therapies for Cancer. J Med Chem 53:6811–6824. doi: 10.1021/jm100509v

15. Varghese B, Vlashi E, Xia W, Ayala Lopez W, Paulos CM, Reddy J, Xu L-C, Low PS (2014) Folate Receptor-β in Activated Macrophages: Ligand Binding and Receptor Recycling Kinetics. Mol Pharmaceutics 11:3609–3616. doi: 10.1021/mp500348e

16. Thomas M, Kularatne SA, Qi L, Kleindl P, Leamon CP, Hansen MJ, Low PS (2009) Ligand-Targeted Delivery of Small Interfering RNAs to Malignant Cells and Tissues. Annals of the New York Academy of Sciences 1175:32–39. doi: 10.1111/j.1749-6632.2009. 04977.x

17. Shen J, Chelvam V, Cresswell G, Low PS (2013) Use of Folate-Conjugated Imaging Agents To Target Alternatively Activated Macrophages in a Murine Model of Asthma. Mol Pharmaceutics 10:1918–1927. doi: 10.1021/mp3006962

18. Dennis MS, Jin H, Dugger D, Yang R, McFarland L, Ogasawara A, Williams S, Cole MJ, Ross S, Schwall R (2007) Imaging tumors with an albumin-binding Fab, a novel tumor-targeting agent. Cancer Res 67:254–261 . doi: 10.1158/0008-5472.CAN-06-2531

19. Borsi L, Balza E, Bestagno M, Castellani P, Carnemolla B, Biro A, Leprini A, Sepulveda J, Burrone O, Neri D, Zardi L (2002) Selective targeting of tumoral vasculature: comparison of different formats of an antibody (L19) to the ED-B domain of fibronectin. Int J Cancer 102:75–85. doi: 10.1002/ijc.10662

20. Adem YT, Schwarz KA, Duenas E, Patapoff TW, Galush WJ, Esue O (2014) Auristatin Antibody Drug Conjugate Physical Instability and the Role of Drug Payload. Bioconjugate Chem 25:656–664. doi: 10.1021/bc400439x

21. Liu X, Guo J, Han S, Yao L, Chen A, Yang Q, Bo H, Xu P, Yin J, Zhang Z (2012) Enhanced immune response induced by a potential influenza A vaccine based on branched M2e polypeptides linked to tuftsin. Vaccine 30:6527–6533. doi: 10.1016/j.vaccine.2012.08.054

22. Jeannin P, Delneste Y, Buisine E, Le Mao J, Didierlaurent A, Stewart GA, Tartar A, Tonnel A-B, Pestel J (1993) Immunogenecity and antigenicity of synthetic peptides derived from the mite allergen Der p I. Molecular Immunology 30:1511–1518. doi: 10.1016/0161-5890(93)90459-O

23. Low PS, Henne WA, Doorneweerd DD (2008) Discovery and Development of Folic-Acid-Based Receptor Targeting for Imaging and Therapy of Cancer and Inflammatory Diseases. Acc Chem Res 41:120–129. doi: 10.1021/ar7000815

24. Hillier SM, Maresca KP, Lu G, Merkin RD, Marquis JC, Zimmerman CN, Eckelman WC, Joyal JL, Babich JW (2013) 99mTc-labeled small-molecule inhibitors of prostate-specific membrane antigen for molecular imaging of prostate cancer. J Nucl Med 54:1369–1376. doi: 10.2967/jnumed.112.116624

25. Ginj M, Zhang H, Waser B, Cescato R, Wild D, Wang X, Erchegyi J, Rivier J, Mäcke HR, Reubi JC (2006) Radiolabeled somatostatin receptor antagonists are preferable to agonists for in vivo peptide receptor targeting of tumors. Proc Natl Acad Sci USA 103:16436–16441. doi: 10.1073/pnas.0607761103

26. Krall N, Pretto F, Decurtins W, Bernardes GJL, Supuran CT, Neri D (2014) A Small-Molecule Drug Conjugate for the Treatment of Carbonic Anhydrase IX Expressing Tumors. Angewandte Chemie International Edition 53:4231–4235. doi: 10.1002/anie.201310709

27. Cazzamalli S, Dal Corso A, Widmayer F, Neri D (2018) Chemically Defined Antibody– and Small Molecule–Drug Conjugates for in Vivo Tumor Targeting Applications: A Comparative Analysis. J Am Chem Soc 140:1617–1621. doi: 10.1021/jacs.7b13361

28. Cazzamalli S, Corso AD, Neri D (2016) Acetazolamide Serves as Selective Delivery Vehicle for Dipeptide-Linked Drugs to Renal Cell Carcinoma. Mol Cancer Ther 15:2926–2935. doi: 10.1158/1535-7163.MCT-16-0283

29. Ghiasikhou S, Marchand A, Zenobi R (2019) A comparative study between a miniaturized liquid junction built in a capillary gap and semi-open capillaries for nL sample infusion to mass spectrometry. Microfluid Nanofluid 23:60. doi: 10.1007/s10404-019-2229-7

30. Neu V, Steiner R, Müller S, Fattinger C, Zenobi R (2013) Development and Characterization of a Capillary Gap Sampler as New Microfluidic Device for Fast and Direct Analysis of Low Sample Amounts by ESI-MS. Anal Chem 85:4628–4635. doi: 10.1021/ac400186t

31. Ghiasikhou S, da Silva MF, Zhu Y, Zenobi R (2017) The capillary gap sampler, a new microfluidic platform for direct coupling of automated solid-phase microextraction with ESI-MS. Anal Bioanal Chem. doi: 10.1007/s00216-017-0652-8

32. Gasymov OK, Glasgow BJ (2007) ANS Fluorescence: Potential to Augment the Identification of the External Binding Sites of Proteins. Biochim Biophys Acta 1774:403–411. doi: 10.1016/j.bbapap.2007.01.002

33. Friess SD, Zenobi R (2001) Protein structure information from mass spectrometry? Selective titration of arginine residues by sulfonates. Journal of the American Society for Mass Spectrometry 12:810–818. doi: 10.1016/S1044-0305(01)00257-4

34. Slavík J (1982) Anilinonaphthalene sulfonate as a probe of membrane composition and function. Biochim Biophys Acta 694:1–25. doi: 10.1016/0304-4157(82)90012-0

35. Almstedt K, Lundqvist M, Carlsson J, Karlsson M, Persson B, Jonsson B-H, Carlsson U, Hammarström P (2004) Unfolding a folding disease: folding, misfolding and aggregation of the marble brain syndrome-associated mutant H107Y of human carbonic anhydrase II. J Mol Biol 342:619–633. doi: 10.1016/j.jmb.2004.07.024

36. Pawliszyn J (2003) Sample preparation: Quo Vadis? Analytical Chemistry 75:2543–2558. doi: 10.1021/ac034094h

37. Motlagh S, Pawliszyn J (1993) On-line monitoring of flowing samples using solid phase microextraction-gas chromatography. Analytica Chimica Acta 284:265–273. doi: 10.1016/0003-2670(93)85310-G

38. Górecki T, Yu X, Pawliszyn J (1999) Theory of analyte extraction by selected porous polymer SPME fibres†. Analyst 124:643–649. doi: 10.1039/A808487D

39. Chapron DJ, Gomolin IH, Sweeney KR (1989) Acetazolamide blood concentrations are excessive in the elderly: propensity for acidosis and relationship to renal function. J Clin Pharmacol 29:348–353. doi: 10.1002/j.1552-4604.1989.tb03340.x